Interferometric Seismic Imaging of Sparsely-sampled Data

Paul Sava, Colorado School of Mines

Summary

Micro-seismicity induced by fluid migration can be used to monitor the migration of fluids during reservoir production and hydro-fracturing operations. The seismicity is usually monitored with sparse networks of seismic sensors. The sparsity of the sensor networks degrades the accuracy of the estimated event locations. This inaccuracy often makes it impossible to infer the fluid pathways at the desired accuracy. Micro-seismicity can be located using an imaging approach based on wave-equation imaging under the exploding reflector model. This idea in itself is not new. What is new, however, is the use of an interferometric imaging algorithm which suppresses artifacts in the location of targets (micro-seismic) and create crisper images, which translates into more accurate location estimates. The images produced with the interferometric imaging method can be used for robust automatic location of micro-earthquakes with application to 4D monitoring of fluid injection.

Introduction

Seismic imaging based on the single scattering assumption (Born approximation) consists of two main steps: wavefield reconstruction, in which step we propagate the recorded wavefields from the acquisition surface into the subsurface, followed by the application of an imaging condition highlighting locations where back-scattering occurs, i.e. where reflectors are present. This framework holds both when the source of seismic waves is located in the subsurface and the imaging target consists of locating this source, as well as when the source of seismic waves is located on the acquisition surface and the imaging target is consists of locating the places in the subsurface where scattering occurs. For simplicity, in this paper I concentrate on the case of imaging active sources located in the subsurface, although the methodology discussed here applies equally well for the more conventional imaging with artificial sources.

Micro-earthquakes can be located using several methods including double-difference algorithms (Waldhauser and Ellsworth, 2000), Gaussian-beam migration (Rentsch et al., 2004), diffraction stacking (Gajewski et al., 2007) or reverse-time migration (Gajewski and Tessmer, 2005). Microearthquake location using reverse-time migration, which is also the technique advocated in this paper, follows the same general pattern mentioned in the preceding paragraph: wavefield-reconstruction backward in time followed by an imaging condition extracting the image (location of the event) at time t=0. The main difficulty with this procedure is that the onset of the micro-earthquake is unknown, i.e. time t=0 is unknown, so the imaging condition cannot be simply applied as it is usually done in zero-offset migration. Instead, an automatic search needs to be performed in the back-propagated wavefield to identify the locations where wavefield energy focuses. This process is complicated and ambiguous since false focusing locations might exist.

This problem is further complicated if the acquisition array is sparse, e.g. when receivers are located in a borehole. In this case, the sparsity of the array itself leads to artifacts in the reconstructed wavefield which might make the automatic picking of focused events even harder. Ideally, the imaging procedure should reduce the artifacts caused by the sparse array to enable robust automatic event picking. Such an imaging procedure is the topic of this paper

Conventional imaging condition

One of the main goals of imaging with active sources is to localize the source of seismic waves. Assuming data $D(\mathbf{x}, t)$ acquired at coordinates $\mathbf{x}=\{x_r,y_r,z_r\}$, e.g. in a borehole, we can reconstruct the wavefield $V(\mathbf{x},\mathbf{y},t)$ at coordinates $\mathbf{y}=\{x,y,z\}$ in the imaging volume using the appropriate Green's function $G(\mathbf{x},\mathbf{y},t)$ corresponding to the locations $\mathbf{x}$ and $\mathbf{y}$:

$$V(\mathbf{x},\mathbf{y},t) = D(\mathbf{x},t) *_t G(\mathbf{x},\mathbf{y},t) \tag{1}$$

where t represents time. The total wavefield $U(\mathbf{y},t)$ at coordinates $\mathbf{y}$ due to data recorded at all receivers $\mathbf{x}$ is

$$U(\mathbf{y},t) = \int_{\mathbf{x}} d\mathbf{x}\, V(\mathbf{x},\mathbf{y},t) \tag{2}$$

A conventional imaging condition (CIC) applied to this reconstructed wavefield extracts the image $R_{CIC}(\mathbf{y})$ as the wavefield at time t=0

$$R_{CIC}(\mathbf{y}) = U(\mathbf{y}, t=0) \tag{3}$$

This imaging procedure succeeds if several assumptions are fulfilled: first, the velocity model used for imaging has to be accurate; second, the numeric solution to the wave-equation used for wavefield reconstruction has to be accurate; third, the data needs to be sampled densely and uniformly on the acquisition surface. Here, I assume that only the third assumption is not fulfilled. In this case, the imaging is not accurate because contributions to the reconstructed wavefield from the receiver coordinates do not cancel-out and lead to imaging artifacts. This situation is analogous to the case of imaging with an inaccurate velocity model, e.g. imaging with a smooth approximation to a random model.

Interferometric imaging condition

One possible solution to reducing random imaging artifacts is to use an interferometric imaging condition (IIC) (Sava and Poliannikov, 2008). In this case, the imaging framework remains the same, e.g. wavefields are reconstructed from all receiver positions using the appropriate Green's functions, equations 1-2. However, IIC does not use for imaging the reconstructed wavefield directly, but a filtered wavefield using pseudo Wigner distribution functions (WDF) (Wigner, 1932) By definition, the pseudo WDF of the reconstructed wavefield $U(\mathbf{y}, t)$ is

$$W(\mathbf{y},t) = \int_{|t_h|\le T} dt_h \int_{|\mathbf{y}_h|\le \mathbf{Y}} d\mathbf{y}_h U\left(\mathbf{y} - \frac{\mathbf{y}_h}{2}, t - \frac{t_h}{2}\right) U\left(\mathbf{y} + \frac{\mathbf{y}_h}{2}, t + \frac{t_h}{2}\right) \tag{4}$$

where $\mathbf{Y}$ and T denote averaging windows in space and time, respectively. Then, the image $R_{IIC}(\mathbf{y})$ is obtained by extracting the time t=0 from the pseudo WDF, $W(\mathbf{y},t)$, of the wavefield $U(\mathbf{y},t)$:

$$R_{IIC}(\mathbf{y}) = W(\mathbf{y}, t=0) \tag{5}$$

As discussed in detail by Sava and Poliannikov (2008), the IIC effectively reduces the artifacts caused by the random fluctuations in the wavefield. Here, I use this imaging condition to attenuate noise caused by data sampling and not noise caused by random velocity variations. However, in principle, IIC addresses both problems at once, since it does not distinguish between the causes of random fluctuations.

Example

I exemplify the interferometric imaging condition method with a synthetic example simulating the acquisition geometry of the passive seismic experiment performed at the San

Andreas Fault Observatory at Depth (SAFOD) (Chavarria et al., 2003). This numeric experiment simulates waves propagating from a source located in the fault zone, e.g. a micro-earthquake, which is recorded in a deviated well located at a distance from the fault, as shown in figure 1(a). For the imaging procedure described in this paper, the micro-earthquake represents the active seismic source. This experiment uses acoustic waves, corresponding to the situation in which we use the P-wave mode recorded by the three-component receivers located in the borehole, figure 1(b). The goal of this experiment is to locate the source position by focusing recorded data using dense and sparse acquisition arrays.

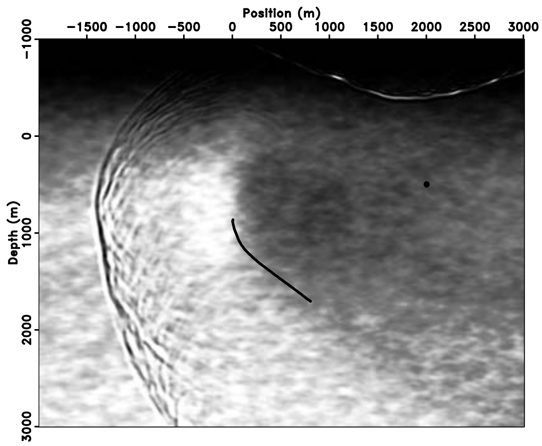

(a)

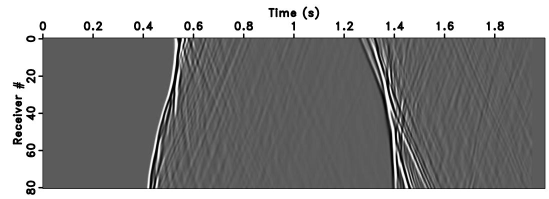

(b)

Figure 1: Velocity model and wavefield snapshot superimposed by the acquisition array and source position (a). Data acquired in the borehole (b).

Figures 2(a)-2(d) show imaging results using various imaging conditions and acquisition geometries. Figures 2(a) and 2(b) are constructed with the conventional imaging condition (CIC), equation 3, while figures 2(c) and 2(d) are constructed using the interferometric imaging condition (IIC), equations 4-5. Both the CIC and IIC images constructed from densely sampled data, figures 2(a)-2(c) localize the source of seismic waves accurately with minor aperture artifacts. However, the CIC image constructed from sparsely sampled data, figure 2(b), shows many imaging artifacts which are only due to the data sampling. In contrast, the IIC image constructed from the same sparsely sampled data, figure 2(d), shows far fewer artifacts and the image is comparable with the similar image obtained using the densely sampled data, figure 2(c).

Conclusions

Interferometric imaging conditions used in conjunction with reverse-time migration reduce artifacts caused by the sparse wavefield sampling on the acquisition array. The images produced by this procedure are crisper and enable robust automatic picking of micro-earthquake location.

Acknowledgment

This research is supported by the sponsors of the Center for Wave Phenomena at Colorado School of Mines.

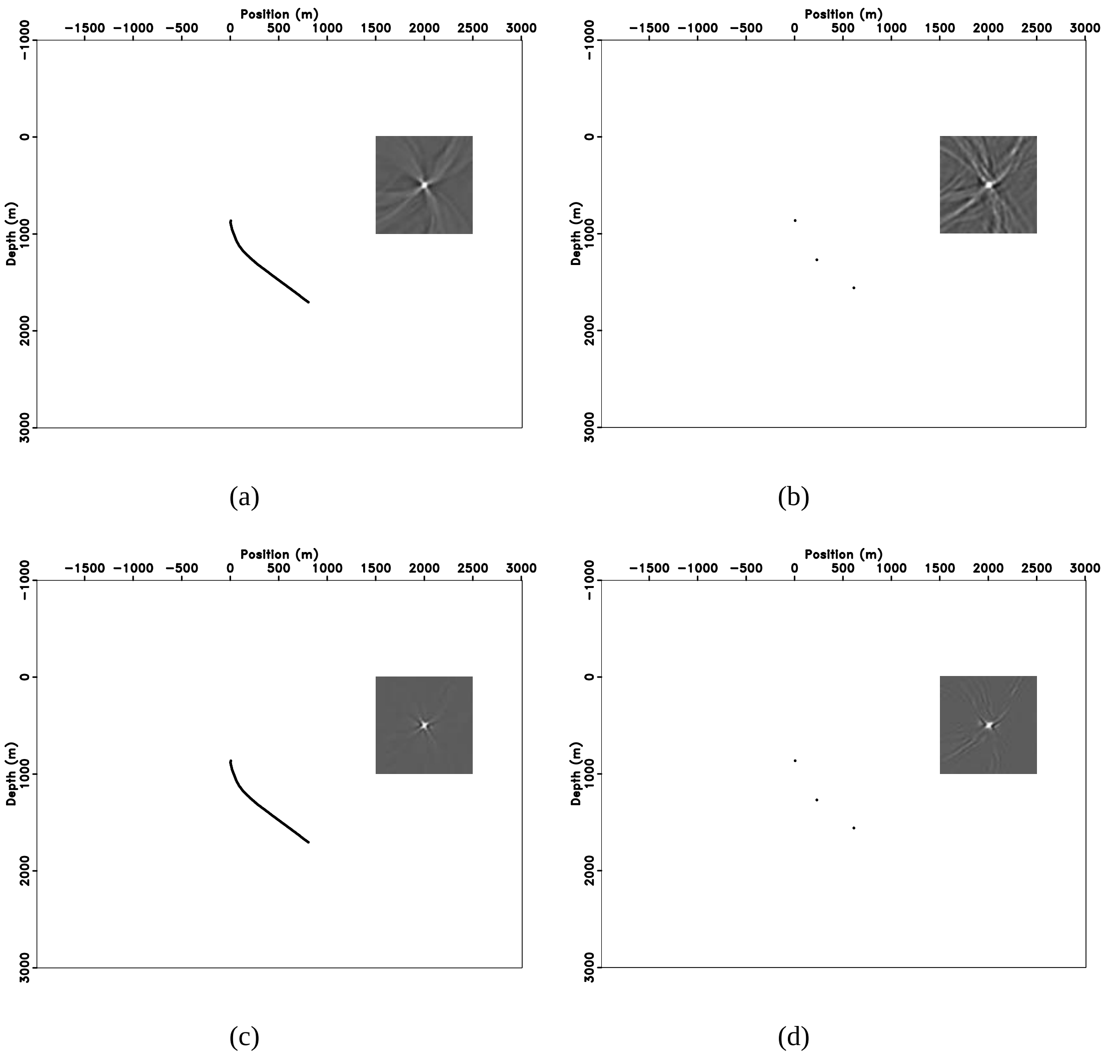

Figure 2: Conventional imaging using dense data sampling (a) and sparse data sampling (b). Interferometric imaging using dense data sampling (c) and sparse data sampling (d).

References

Chavarria, J., P. Malin, R. Catchings, and E. Shalev, 2003, A look inside the San Andreas fault at Parkfield through vertical seismic profiling: Science, **302**, 1746–1748.

Gajewski, D., D. Anikiev, B. Kashtan, E. Tessmer, and C. Vanelle, 2007, Localization of seismic events by diffraction stacking: 76th Annual International Meeting, SEG, Expanded Abstracts, 1287–1291.

Gajewski, D. and E. Tessmer, 2005, Reverse modelling for seismic event characterization: Geophysical Journal International, **163**, 276–284.

Rentsch, S., S. Buske, S. Lth, and S. A. Shapiro, 2004, Location of seismicity using Gaussian beam type migration: 74th Ann. Internat. Mtg., 354–357, Soc. of Expl. Geophys.

Sava, P. and O. Poliannikov, 2008, Interferometric imaging condition for wave-equation migration: Geophysics, in press.

Waldhauser, F. and W. Ellsworth, 2000, A double-difference earthquake location algorithm: Method and application to the northern Hayward fault: Bulletin of the Seismological Society of America, **90**, 1353–1368.

Wigner, E., 1932, On the quantum correction for thermodynamic equilibrium: Physical Review, **40**, 749–759.